JOURNAL OF SYNCHROTRON RADIATION

Volume 23 (2016)

Supporting information for article:

Development of a single-cell x-ray fluorescence flow cytometer

Andrew M. Crawford, Patrick Kurecka, Tsz Kwan Yim, Claire Kozemchak, Aniruddha Deb, Lubos Dostal, Cheng-Jun Sun, Dale L. Brewe, Raul Barrea and James E. Penner-Hahn

Supporting information for

Development of a single-cell x-ray fluorescence flow cytometer

Andrew M. Crawford, Patrick Kurecka, Tsz Kwan Yim, Claire Kozemchaa, Aniruddha Deb, Lubos Dostal, Cheng-Jun Sun, Dale L. Brewe, Raul Barrea and James E. Penner-Hahn

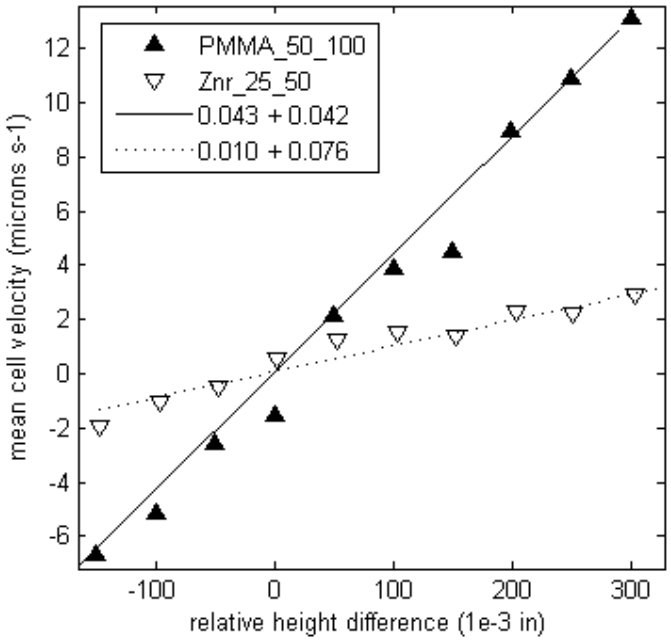

Figure S1. Syphon Pump Tests. Cellular velocities of two different capillaries as a function of the relative height difference of the two ends of the syphon pump. PMMA, polymethylmethacrylate (50 μm i.d., 100 μm o.d.; Znr, Zeonor® (25 μm i.d., 50 μm o.d.)

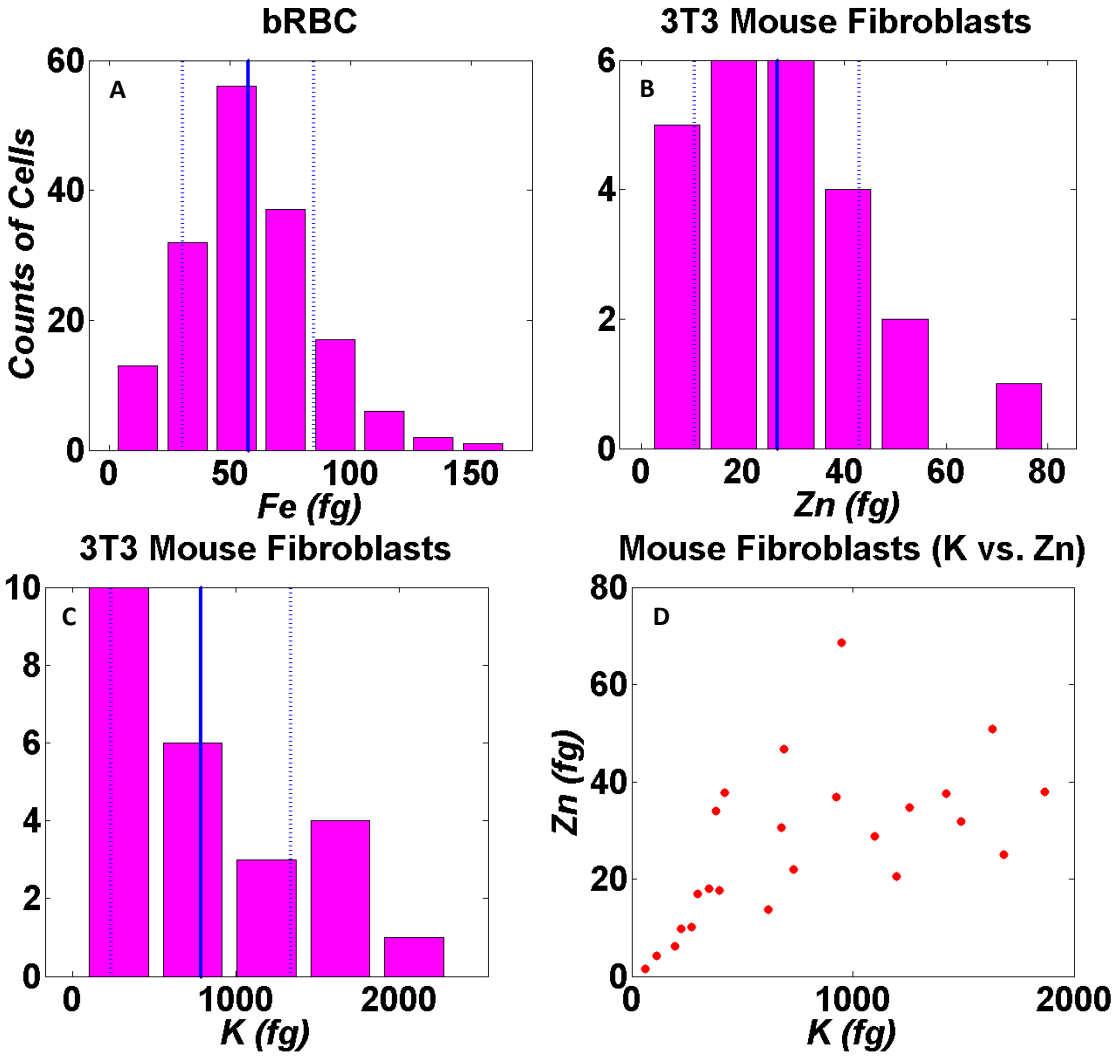

Figure S2. Experimentally determined elemental distributions. A-C are histograms of observed mass distributions for different elements and different cell types with cell counts shown as pink bars, mean concentrations shown a blue solid line,a nd standard deviation marked by blue dashed lines. (A) Fe content in bovine RBCs; (B) Zn content in NIH3T3 mouse fibroblasts; (C) K content in NIH3T3 mouse fibroblasts. (D) is a correlation plot of K vs. Zn for individual NIH3T3 mouse fibroblasts.

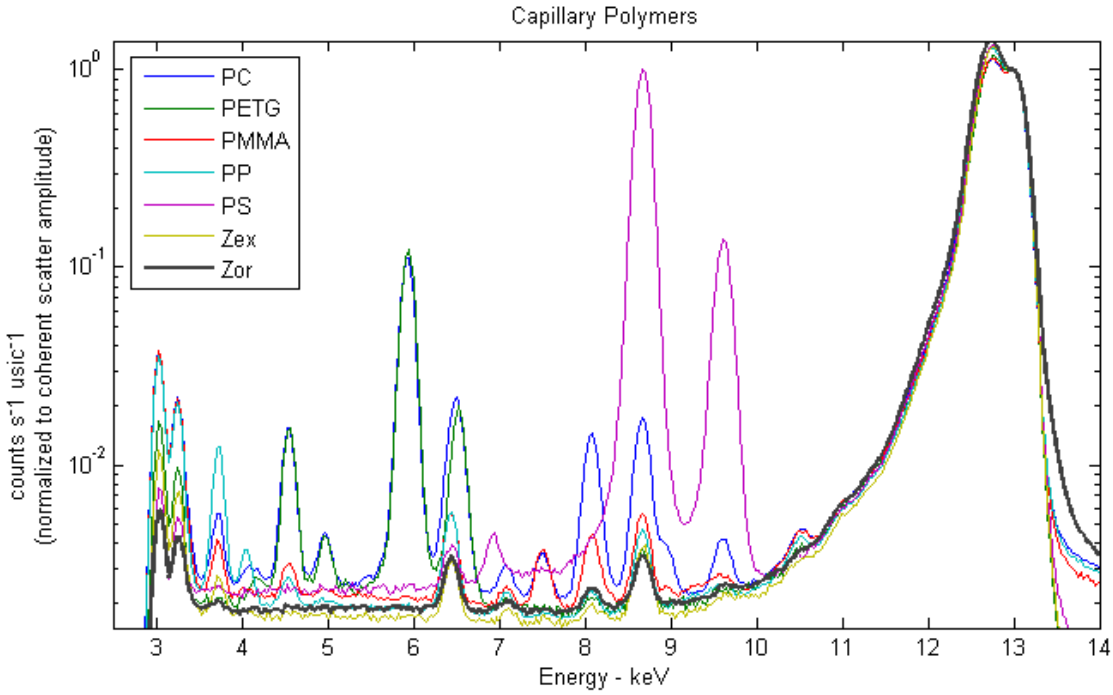

Figure S3. XRF Spectra of Capillary Materials: An overlay of the XRF spectra for different capillary materials, normalized to the elastic scattering amplitude at 13 keV. PC – Polycabonate; PETG - Polyethylene Terephtalate Glycol-modified; PMMA – Polymethylmethacrylate; PP – Polypropylene; PS – Polystyrene; Zex – Zeonex; Zor – Zeonor.

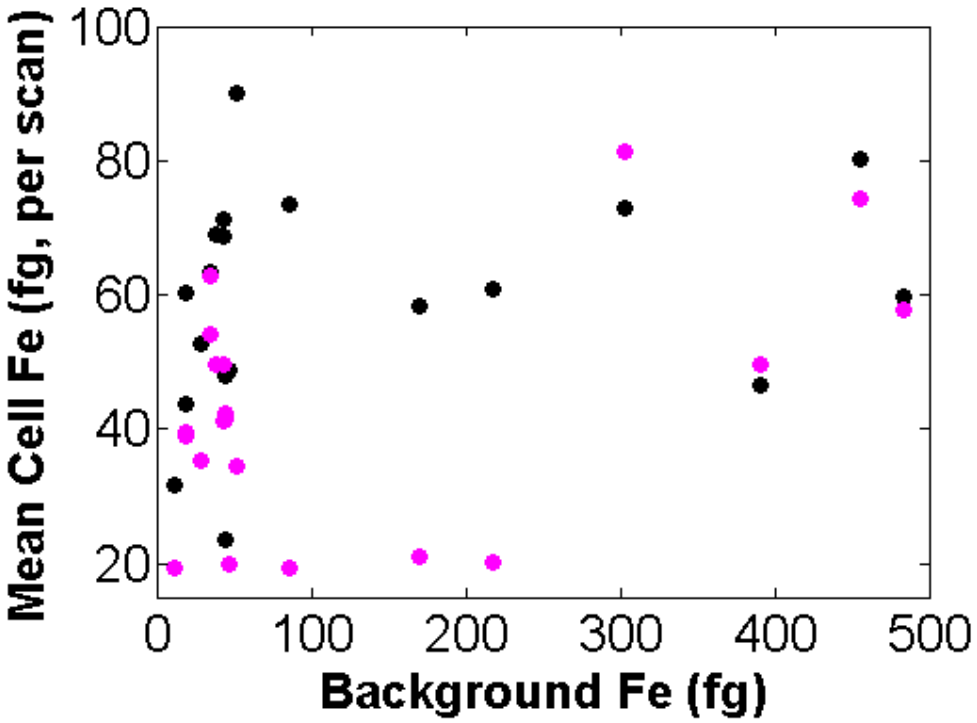

Figure S4. Dependence of apparent Fe concentration on the level of capillary contamination. Each point represents the average of the data for all of the cells measured during a single 10-minute cytometer scan. The mean (black) and std. deviation (pink) of Fe concentration for each scan is plotted vs. the background Fe contamination for that segment of the capillary.. The apparent cell composition does not depend on the level of background impurity, confirming the accuracy of the background removal. However, the uncertainty in each measurement (pink circles) is noticeably larger relative to the mean at high background levels, reflecting the noise associated with background removal when the background signal is significantly larger than the cell signal.

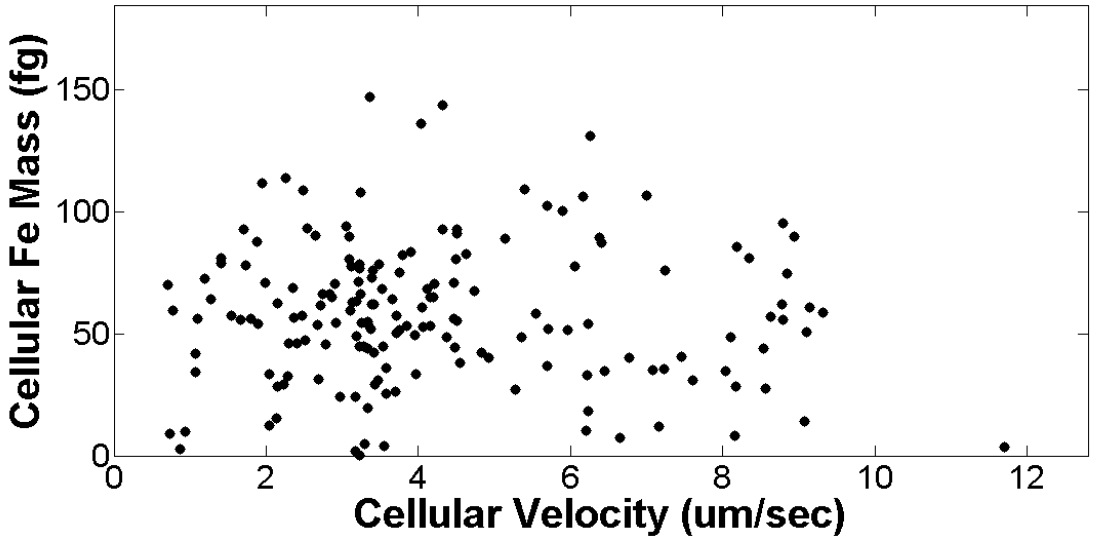

Figure S5. Dependence of apparent Fe concentration on velocity. For each bovine RBC, the apparent Fe composition is compared with the mean cellular velocity during XRF measurement. The absence of any dependence on velocity confirms the accuracy of the time-to-space conversion during mass calculation (section 3.2).

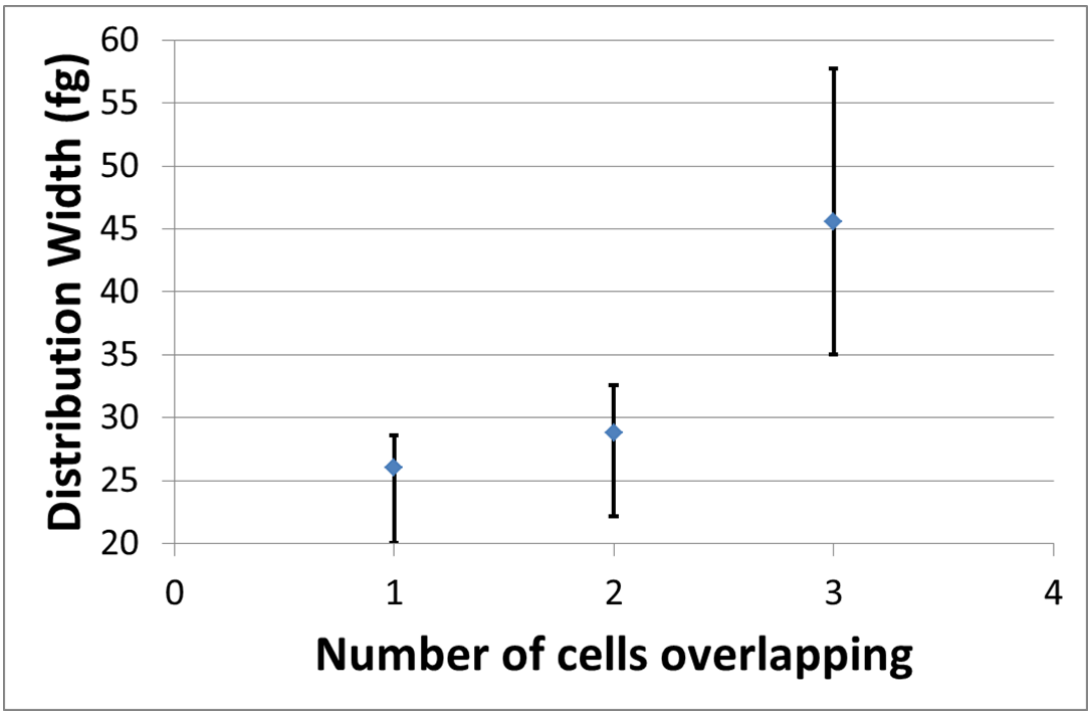

Figure S6. Dependence of apparent Fe composition on the extent of cell overlap. The bRBC cells were segregated into groups with one, two, or three cells in the beam at one time and the standard deviation in the apparent Fe composition was determined for each sub-population. The data plotted are the standard deviation (blue point) and the 80% confidence limits for each distribution. The population with two overlapping cells is indistinguishable from that for single cells, suggesting that the deconvolution algorithm can effectively handle 2 overlapping cells. In contrast, three overlapping cells show a much larger apparent standard deviation, indicating that the metal is not properly apportioned between cells.